ELSEVIER

Biochimica et Biophysica Acta 1567 (2002) 193–203

BIOCHIMICA ET BIOPHYSICA ACTA
BBA

www.bba-direct.com

Ion transport across a phospholipid membrane mediated by the peptide trichogin GA IV

T.N. Kropacheva[a], J. Raap[b,*]

[a] *Department of Chemistry, Udmurt State University, Izhevsk, Russia*
[b] *Leiden Institute of Chemistry, Gorlaeus Laboratories, Leiden University, P.O. Box 9502, 2300 RA Leiden, The Netherlands*

Received 26 April 2002; received in revised form 22 July 2002; accepted 26 September 2002

Abstract

Trichogin GA IV is a special member of a class of peptaibols that are linear peptide antibiotics of fungal origin, characterised by the presence of a variable number of α-aminoisobutyric acid residues, an acyl group at the N-terminus and a 1,2-amino alcohol at the C-terminus. Most of the peptaibols display ion-channel-forming or at least membrane-modifying properties. The 11-residue-long trichogin GA IV is not only one of shortest peptaibols, but it is also unique for its *n*-octanoyl group instead of the more common found acetyl group at the N-terminus. For the first time we have found that this lipopeptaibol is able to enhance conduction of monovalent cations through membranes of large unilamellar vesicles (LUVs). The influence of the [Leu-OMe]trichogin GA IV analogue (TRI) on ion permeation was studied under a variety of conditions (lipid composition, lipid-to-peptide ratio and a transmembrane potential). Parallel experiments were performed with the 16-residue long, channel-forming peptaibol, zervamicin (ZER). For the two peptides, the permeability between K^+ and Na^+ was found to be different. In addition, the ion diffusion rate dependencies on the peptide concentration are observed to be different. This might indicate that a different number of aggregated molecules are involved in the rate-limiting step, i.e. 3–4 (TRI) and 4–7 (ZER). In the presence of TRI, dissipation of the transmembrane potential, $\Delta\psi$, was observed with a rate to be dependent on the magnitude of both initial $\Delta\psi$ and peptide concentration. Both peptides were activated by a *cis*-positive but not by *cis*-negative $\Delta\psi$. Under identical conditions the ion-conducting efficiency of zervamicin was 100–200 times higher than that of trichogin. Our results show that, unlike for zervamicin, the membrane-modifying activity of trichogin is not associated with a channel mechanism.

Keywords: Ion permeation; Peptaibol; Trichogin; Zervamicin; Large unilamellar vesicle; Transmembrane potential

1. Introduction

Peptaibols, such as alamethicin, suzukacilin, trichorzianin, zervamicin, antiamoebin, trichogin, etc., are linear peptides of fungal origin, characterised by a high content of helix-promoting α-aminoisobutyric acid residues, an acylated N-terminus and a 1,2-amino alcohol at the C-terminus (Table 1). Many peptaibol antibiotics display ion channel forming properties and can serve as good model systems for a better understanding of the function of complex channel proteins. One of the longest and best studied peptaibols is the 20-residue-long alamethicin (reviewed in Refs. [1–6]). Natural alamethicin (a mixture of several close related analogues) forms voltage-gated ion channels in a variety of lipid membranes with discrete conductance multilevels. It is generally accepted that the channels are formed by aggregation of a variable number of amphipathic helices into transmembrane bundles.

Zervamicins belong to another family of peptaibols, i.e. 16-residue antibiotic peptides isolated from *Emericellopsis salmosynnemata* [7]. The major component of the zervamicin analogues, zervamicin IIB (Table 1), shows almost the same ion conducting properties as alamethicin [8,9]. The voltage-induced conductance is asymmetric with a higher current observed at *cis*-positive potentials compared to that at a *cis*-negative voltage [4,5,9,10]. The zervamicin structure in the crystal state and solution is also typical for that of peptaibols [11–13]. The amphipathic helical structure has a well-pronounced polar face, which can line the interior of the channel.

Abbreviations: ALA, alamethicin; GRA, gramicidin; LUVs, large unilamellar vesicles; PC, L-α-phosphatidylcholine; PG, L-α-phosphatidyl-DL-glycerol; TRI, trichogin GA IV; VAL, valinomycin; ZER, zervamicin

* Corresponding author. Tel.: +31-71-527-4419; fax: +31-71-527-4537.

E-mail address: J.Raap@chem.leidenuniv.nl (J. Raap).

0005-2736/02/$ - see front matter © 2002 Elsevier Science B.V. All rights reserved.
PII: S0005-2736(02)00616-8

Table 1
Amino acid sequence of selected peptaibols

Alamethicin (R_f=30)	Ac-Aib^1-Pro^2-Aib^3-Ala^4-Aib^5-Ala^6(Aib^6)-Gln^7-Aib^8-Val^9-Aib^{10}-Gly^{11}-Leu^{12}-Aib^{13}-Pro^{14}-Val^{15}-Aib^{16}-Aib^{17}-Glu^{18}-Gln^{19}-Phl^{20}
Alamethicin (R_f=50)	Ac-Aib^1-Pro^2-Aib^3-Ala^4-Aib^5-Ala^6(Aib^6)-Gln^7-Aib^8-Val^9-Aib^{10}-Gly^{11}-Leu^{12}-Aib^{13}-Pro^{14}-Val^{15}-Aib^{16}-Aib^{17}-Gln^{18}-Gln^{19}-Phl^{20}
Zervamicin IIA	Ac-Trp^1-Ile^2-Gln^3-Aib^4-Ile^5-Thr^6-Aib^7-Leu^8-Aib^9-Hyp^{10}-Gln^{11}-Aib^{12}-Hyp^{13}-Aib^{14}-Pro^{15}-Phl^{16}
Zervamicin IIB	Ac-Trp^1-Ile^2-Gln^3-Iva^4-Ile^5-Thr^6-Aib^7-Leu^8-Aib^9-Hyp^{10}-Gln^{11}-Aib^{12}-Hyp^{13}-Aib^{14}-Pro^{15}-Phl^{16}
Leu-Zervamicin	Ac-Leu^1-Ile^2-Gln^3-Iva^4-Ile^5-Thr^6-Aib^7-Leu^8-Aib^9-Hyp^{10}-Gln^{11}-Aib^{12}-Hyp^{13}-Aib^{14}-Pro^{15}-Phl^{16}
Trichogin GA IV	*n*-Oct-Aib^1-Gly^2-Leu^3-Aib^4-Gly^5-Gly^6-Leu^7-Aib^8-Gly^9-Ile^{10}-Lol^{11}
[LeuOMe] Trichogin GA IV	*n*-Oct-Aib^1-Gly^2-Leu^3-Aib^4-Gly^5-Gly^6-Leu^7-Aib^8-Gly^9-Ile^{10}-Leu-OMe^{11}

n-Oct = *n*-octanoyl; Phl = L-phenylalaninol; Lol = L-leucinol; Aib = α-aminoisobutyric acid.

The total length of the zervamicin helix is about 26–29 Å, which is enough to span the hydrophobic core of the bilayer (~ 30 Å). Thus, similar to alamethicin, the membrane activity of zervamicin is likely associated with the formation of voltage-gated channels via a barrel-stave mechanism.

One of the shortest peptaibol antibiotics is the 11-residue-long trichogin GA IV (Table 1) isolated from the cultures of *Trichoderma longibrachiatum* [14]. This so-called lipopeptaibol is characterised by a lipophilic group attached to the N-terminus [15]. Similar to the longer peptaibols, trichogin GA IV exhibits a helical structure with the hydrophilic face comprised of only four glycine residues. In spite of its shorter length (~ 16 Å), trichogin shows considerable membrane-modifying activity [14–17]. However, the long axis of the trichogin helix was oriented parallel to the membrane surface [17] and it was concluded that the most likely mode of trichogin action (at least in the absence of a transmembrane potential) is according to a "carpet-like" mechanism [18,19].

The present paper aimed at the study of the membrane activity of the synthetic [Leu^{11}OMe]trichogin GA IV analogue (Table 1), which was shown to have a conformation and activity comparable to that of natural trichogin GA IV [14,16]. Since the trichogin-induced membrane permeation was previously characterised only via carboxyfluorescein leakage, it was of interest to see whether trichogin can also induce permeation of small inorganic ions through a membrane. The transmembrane fluxes of sodium and potassium cations in the presence of trichogin were studied in order to see if there is some discrimination in their transport mechanism often observed in membrane systems [3,20]. The experiments were performed with large unilamellar vesicles (LUVs) prepared from zwitterionic (egg L-α-phosphatidylcholine (PC)) and acidic (egg L-α-phosphatidyl-DL-glycerol (PG)) lipids. Since many peptaibols exhibit potential-dependent behaviour, the influence of the transmembrane potential on the activity of trichogin was also studied. All experiments were performed in comparison with the channel-forming zervamicin to get additional information about the mechanism of trichogin-induced ion conduction.

2. Materials and methods

LUVs were prepared by rapid extrusion of an aqueous egg PC or egg PG (Sigma). A high-pressure extruder with a stack of two membrane polycarbonate filters (Nucleopore, 100-nm pore size) was used as described in Ref. [21]. To determine the internal volume, vesicles were prepared in 200 mM KCl and the external solution was exchanged for 200 mM NaCl by passage of the vesicles through a Sephadex G-50 column. The entrapped K^+ was released by addition of the pore-forming peptide gramicidin D (GRA, Molecular Probes) and its concentration was determined with a K^+-selective electrode (Orion). The trapped volume per mole of PC was found to be 1.2 l, which is close to reported values for PC LUVs produced by extrusion through 100 nm filters [21]. The distribution of vesicle sizes was determined by photon correlation spectroscopy using a Zetasizer 3000 (Malvern Instruments). The *Z*-average size was found to be 90 nm.

The PC concentration was determined by an enzymatic colorimetric method using a commercial kit (PL MRP2; Boehringer Mannheim). The PG content was measured by inorganic phosphate analysis according to Ref. [22].

Zervamicin (ZER, a 1:1 mixture of the closely related analogues zervamicins IIA and IIB) was isolated from the biomass obtained from a culture of *E. salmosynnemata* according to Ref. [23]. [Leu^{11}OMe]trichogin GA IV (TRI), a kind gift of Prof. C. Toniolo, was synthesised as described in Ref. [16]. Small aliquots of a stock solution of peptide in dimethyl sulfoxide (DMSO) were added to the vesicles up to a final concentration of less than 2% DMSO (by volume).

For the imposition of a transmembrane potential, $\Delta\psi$, outside positive vesicles were prepared in solution containing 200 mM KCl and 10 mM Tris·HCl (pH 7.4). For generation of $\Delta\psi$, outside negative vesicles were prepared in 2 mM KCl, 198 mM NaCl and 10 mM Tris·HCl (pH 7.4). To produce K^+ transmembrane gradients, the stock solution was diluted 100-fold into one containing variable concentrations of KCl and NaCl (total concentration 200 mM) and 10 mM Tris·HCl (pH 7.4). Generation of $\Delta\psi$ by addition of valinomycin (VAL, Sigma) to vesicles was followed with the potential-sensitive probes safranine T (SAF, Riedel-de-Haen) and oxonol VI (OXO, Molecular Probes).

For K^+- or Na^+-uptake studies, vesicles were prepared in 200 mM Me_4NCl, 10 mM Tris·HCl (pH 7.4) in the presence of the ~ 50 μM potassium benzofuran isophtalate (PBFI, Molecular Probes). The unbound indicator was removed by passage through a Sephadex G-50 column pre-equilibrated with the same buffer (except for the indicator). The solution

was diluted 50–100 times into the medium containing different amounts of KCl (NaCl), Me_4NCl (total concentration 200 mM) and 10 mM Tris·HCl (pH 7.4).

Fluorescence was measured with a Perkin-Elmer luminescence spectrofluorimeter LS50 B. The absorption spectra were obtained with a Perkin-Elmer Lambda 900 UV/VIS/NIR spectrophotometer. All experiments were performed at room temperature (20 ± 1 °C).

3. Results

3.1. Binding of peptide to PC vesicles

To study the peptide-to-lipid binding, the intrinsic fluorescence of ZER (due to the presence of the Trp^1 residue) was examined under different conditions. In aqueous solution the maximum of the ZER emission spectrum is at 360 nm. Upon addition of PC vesicles (L:P < 1) the intensity of fluorescence decreases without changing the emission band position (Fig. 1). Further addition of lipid results into a gradual shift of the emission band to 340 nm. The titration curve (Fig. 1, inset) shows a fast saturation at L:P ~ 5. This result indicates that, under the conditions used in our experiments described below (L:P>1000) ZER molecules bind quantitatively to the membrane.

The affinity of TRI for phospholipid vesicles cannot be determined in the way described above. However, due to the lipophilic nature of TRI, its binding to vesicles is expected to be even stronger.

The blue shift of ZER fluorescence (362 → 341 nm) upon binding to vesicles (Fig. 1A) indicates an increase in hydrophobicity of the environment at the N-terminus of the peptide. For comparison, the position of the maximum of

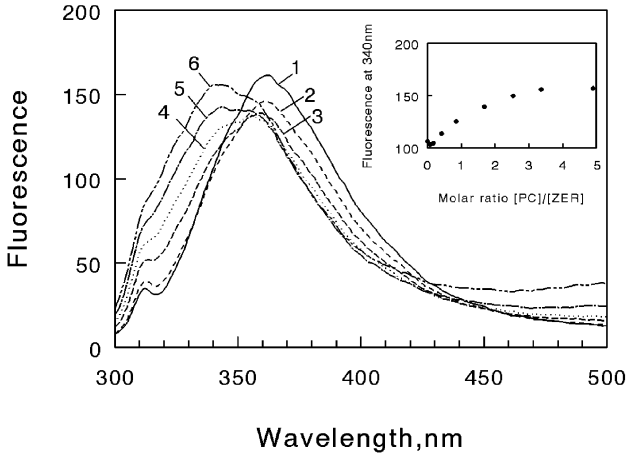

Fig. 1. Fluorescence emission spectrum of ZER (C_{ZER} = 0.66 μM) in aqueous solution containing 200 mM KCl and 10 mM Tris·HCl (pH 7.4) (curve 1) and in the presence of variable amounts of PC vesicles (loaded with the same buffer), i.e. C_{PC} = 0.06 μM (curve 2); 0.28 μM (3); 0.56 μM (4); 1.11 μM (5); 2.22 μM (6). λ_{ex} = 280 nm. Inset: fluorescence intensity at λ_{max} = 340 nm upon titration with PC vesicles.

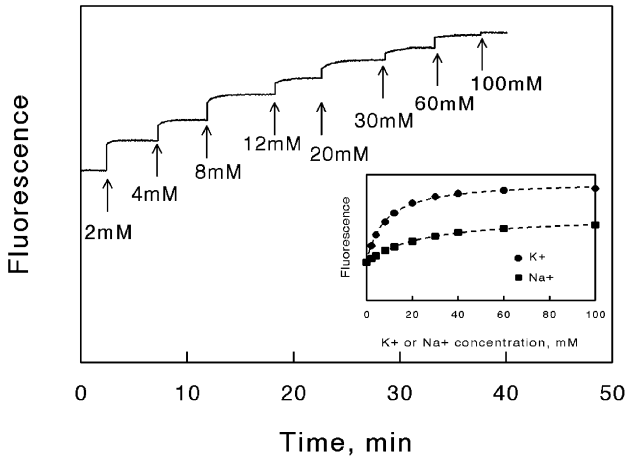

Fig. 2. Calibration of the PBFI fluorescence emission. To PC vesicles, loaded with ~ 50 μM PBFI in 200 mM $(CH_3)_4NCl$, 10 mM Tris·HCl (pH 7.4) with the same external medium (except of PBFI), small aliquots of KCl were added to indicated final concentrations in the presence of GRA (3 μM). C_{PC} = 213 μM; λ_{ex} = 340 nm, λ_{em} = 525 nm; 430 nm cut-off filter. Inset: PBFI fluorescence emission as a function of K^+ and Na^+ concentrations.

fluorescence was measured in a number of solvents of decreased polarity, i.e. λ_{max} = 362 nm (water, ϵ = 79), 356 nm (DMSO, ϵ = 47), 343 nm (methanol, ϵ = 33), 340 nm (CH_2Cl_2, ϵ = 9) and 340 nm (*n*-hexane, ϵ = 2). Thus, the fluorescence maximum at 341 nm for vesicle-bound ZER may correspond to penetration of the N-terminal Trp^1-residue into the hydrophobic core of the membrane (ϵ = 2–4).

3.2. Peptide-mediated K^+- and Na^+-influx

In order to monitor the peptaibol-mediated potassium (or sodium) influx, the encapsulated fluorescent indicator PBFI was employed. Preliminarily, the spectral response of PBFI to intravesicular K^+ was determined by a standard procedure [24]. To PC (or PG) LUVs, loaded with the indicator, increasing amounts of KCl were added in the presence of the pore-forming antibiotic GRA (Fig. 2). The increase of fluorescence was analysed to determine the dissociation constant (K_d) of the indicator–cation complex (Fig. 2, inset). Under our experimental conditions, the K_d values of PBFI determined for K^+ are 7.8 mM (PC LUVs) and 7.6 mM (PG LUVs).

Although PBFI was primary designed as a fluorescent indicator for K^+, it can also be used to monitor the Na^+ concentrations (see inset in Fig. 2) [25]. The dissociation constants of the PBFI–Na^+ complex for different types of phospholipids are 23.4 mM (PC LUVs) and 15.4 mM (PG LUVs). The concentration range over which the maximum sensitivity of the indicator corresponds to approximately 1–40 mM of K^+ (Na^+).

The peptide-mediated K^+ uptake into vesicles was studied by measuring the fluorescence of encapsulated PBFI as a function of time upon addition of appropriate amounts

of peptide in the presence of a K^+-transmembrane gradient (Fig. 3A). No increase of PBFI fluorescence is observed in the absence of peptide, which indicates that the PC membrane is highly impermeable to K^+ ions. Upon addition of TRI, an initial steep increase of PBFI fluorescence is observed due to the rapid influx of K^+ ions from the extravesicular space. A further leakage of K^+ ions is sped down since it becomes tightly coupled to a counterflow of Me_4N^+ ions, so that the slower phase of the fluorescence curves depends on the rate of TRI-mediated K^+/Me_4N^+

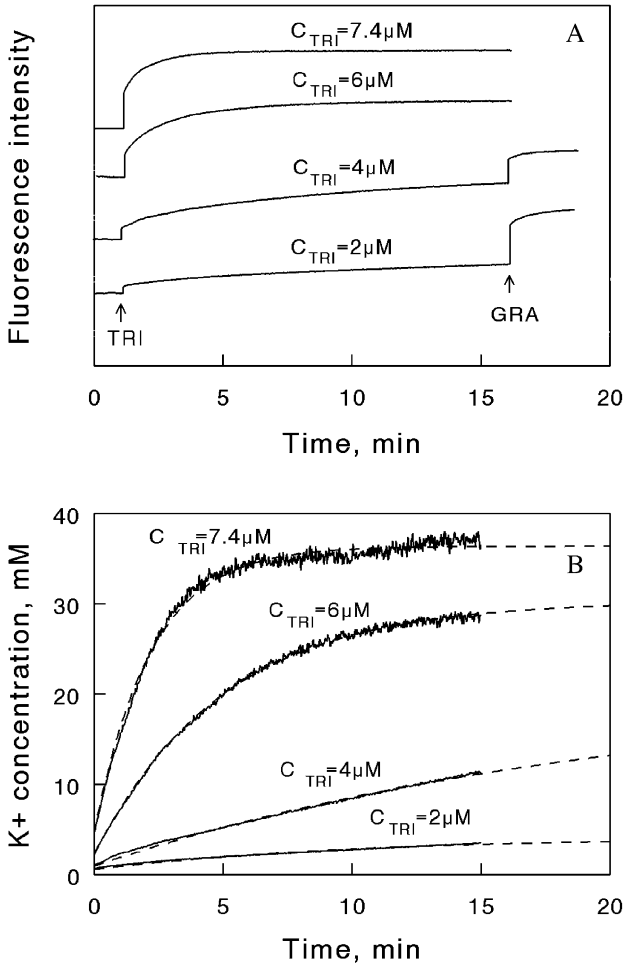

Fig. 3. (A) Time dependence of PBFI fluorescence emission upon additions of different amounts of TRI to PC vesicles. The vesicles were loaded inside with ~ 50 μM PBFI, 200 mM $(CH_3)_4NCl$, 10 mM Tris·HCl (pH 7.4). The bulk solution (the outside of the vesicles) contained 160 mM $(CH_3)_4NCl$, 40 mM KCl, 10 mM Tris·HCl (pH 7.4). TRI was added to the indicated final concentrations. GRA (2 μM) was used for complete equilibration of K^+ across the membrane. $C_{PC}=213$ μM; $\lambda_{ex}=340$ nm, $\lambda_{em}=525$ nm; 430 nm cut-off filter. (B) The time dependence of intravesicular K^+ concentration upon addition to PC vesicles (at $t=0$) of different amounts of TRI (final concentrations are indicated near each curve). The experimental data shown in panel A were transformed into intravesicular K^+ concentration using the preliminary determined dissociation constant of the indicator–K^+ complex ($K_d=7.8$ mM). The dashed lines represent the best fit of the experimental data with the relationship $C_{in}=C_{out}-(C_{out}-C_{in}^0)\exp(-kt)$. All conditions are the same as in Fig. 2.

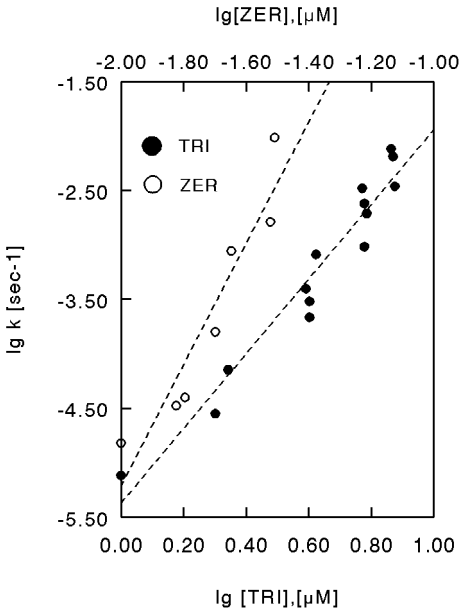

Fig. 4. The K^+/Me_4N^+ exchange diffusion rate constant as a function of TRI or ZER concentrations. The K^+-uptake into PC vesicles was induced by addition of peptides in the presence of a transmembrane gradient with $[K^+]_{in}<[K^+]_{out}$. $C_{PC}=213$ μM.

exchange transport. At the end of each experiment GRA was added to achieve complete equilibration of K^+ concentration across the membrane. The concentration of cations inside the vesicles C_{in} (Fig. 3B) was calculated from the preliminarily determined values of K_d:

$$C_{in}=K_d(I-I_0)/(I_{max}-I)$$

where I is the fluorescence at a given time, I_0 the initial fluorescence, I_{max} the fluorescence upon complete binding with a cation. The initial (at $t\rightarrow 0$) rapid rise of the internal K^+ concentration is followed by a slower phase, which is described by first-order kinetics with respect to the K^+-gradient across the membrane:

$$dC_{in}/dt=k(C_{out}-C_{in})$$

Integration gives the equation for the intravesicular K^+ concentration:

$$C_{in}=C_{out}-(C_{out}-C_{in}^0)\exp(-kt),$$

where C_{in}^0 is the intravesicular K^+ concentration after fast initial influx (at $t\rightarrow 0$). To determine the apparent rate constant of K^+/Me_4N^+ exchange (k), fitting of the experimental data was performed with the floated C_{out} value (Fig. 3B). For low concentrations of TRI, the C_{out} values were lower than the external K^+ concentration, showing that some vesicles were not affected by TRI. At sufficiently high concentrations of TRI, a complete equilibration of $[K^+]_{in}$ and $[K^+]_{out}$ occurred, so that $C_{out}=C_{out}^0$.

Fig. 4 shows the relationship between the cation diffusion rate constant k and peptide concentration. The K^+

uptake mediated by ZER showed a much higher efficiency. Compared to TRI, on the average, a 200-time smaller concentration of ZER is required to get similar values of k. Assuming that the rate constant is proportional to the peptide concentration as: $k \sim [\text{peptide}]^N$, a double logarithmic plot of k versus peptide concentration gives $N = 3.4 \pm 0.4$ for TRI and $N = 5.6 \pm 1.6$ for ZER. Thus, the observed concentration dependence indicates some cooperativity in both the TRI and ZER activities to enhance K^+ transportation.

A comparison of K^+- and Na^+-influx in the presence of peptides was made in parallel experiments with the same vesicle preparation containing encapsulated PBFI with KCl or NaCl as external electrolytes (Fig. 5A–D). The observed differences in K^+ and Na^+ transport across a membrane demonstrate that permeation of Me_4N^+ ions is not rate-limiting. Fig. 5A shows that in PC vesicles the TRI-induced influx is more efficient for K^+ than for Na^+. The calculated ratio of the K^+/Na^+ transport rates for 2 μM TRI shows an about 1.6-time faster transport of K^+ compared to Na^+ (Table 2). For the acidic lipid PG membrane, even without any peptide added, some uptake of K^+, but not of Na^+, was observed (Fig. 5C). This finding is in line with the literature data, which demonstrated that negatively charged lipids facilitate cation diffusion across the membrane while positively charged membranes are highly cation impermeable [26]. At the same concentration of TRI for PG vesicles (Fig. 5C) the difference between K^+ and Na^+ is higher ($k_{K+}/k_{Na+} = 2.9$). However, with further increase of the TRI concentration the discrimination in permeability between K^+ and Na^+ is getting smaller (Table 2).

Table 2
The ratio of rate constants of K^+- and Na^+-transport across the lipid membrane in the presence of peptides

Peptide	k_{K+}/k_{Na+}, PC-membrane	k_{K+}/k_{Na+}, PG-membrane
TRI (2 μM)	1.6	2.9
TRI (4 μM)	1.6	1.5
TRI (6 μM)	1.2	1.3
ZER (0.01 μM)	0.9	1.6
ZER (0.02 μM)	0.6	0.4
ZER (0.03 μM)	0.6	0.5

In the presence of low amounts of ZER (0.01 μM) the PG membrane remains still more permeable to K^+, but upon

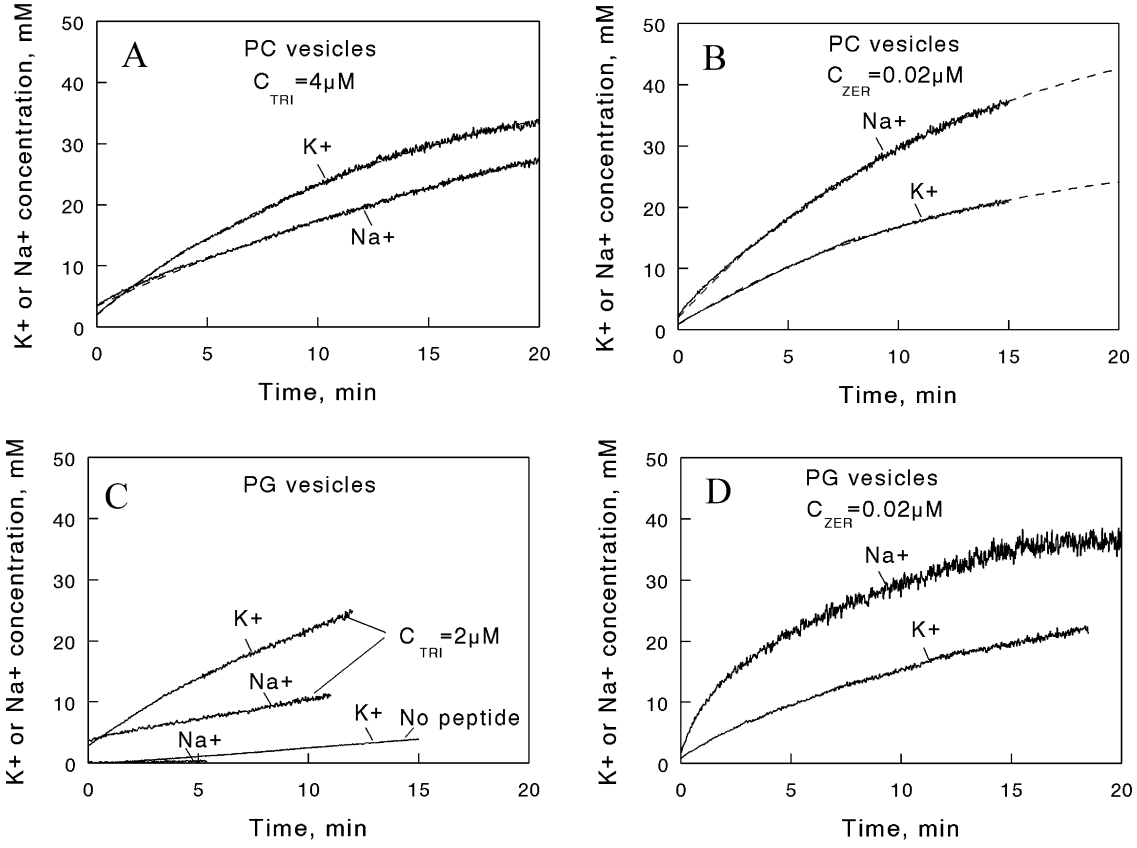

Fig. 5. The time-course of K^+- or Na^+-uptake into pure PG vesicles (two curves at the bottom of panel C) and upon addition of TRI and ZER (at $t = 0$) to PC vesicles (panels A, B) and to PG vesicles (panels C, D). The phospholipid vesicles contained inside 200 mM $(CH_3)_4NCl$, 10 mM Tris·HCl (pH 7.4) and outside 200 mM KCl or NaCl, 10 mM Tris·HCl (pH 7.4). $C_{PC} = 213$ μM; $C_{PG} = 190$ μM. Vesicle-encapsulated PBFI was used as a K^+- and Na^+-sensitive fluorescence indicator.

further addition of ZER (0.02–0.03 μM) the Na^+ influx becomes about two times faster than that of K^+ in both PC and PG vesicles (Fig. 5B and D, Table 2).

3.3. Peptide-induced dissipation of the transmembrane potential

To elucidate the influence of the transmembrane potential $\Delta\psi$ on the ability of TRI to permeate the lipid bilayer, $\Delta\psi$ was installed in LUVs with a K^+ gradient across the membrane by addition of the K^+-ionophore VAL. Generation of $\Delta\psi$ was followed with the potential-sensitive dyes safranine T ($\Delta\psi$, *cis*-positive) [27,28] and oxonol VI ($\Delta\psi$, *cis*-negative) [29,30]. When K^+ is the only diffusing ion, the magnitude of the installed $\Delta\psi$ is given by the Nernst equation:

$$\Delta\psi = (RT/F)\ln([K^+_{in}]/[K^+_{out}]).$$

The sign of $\Delta\psi$ refers to the extravesicular solution, which is the *cis*-phase with respect to the added peptide. When VAL was added to the vesicle dispersion with $[K^+_{in}]>[K^+_{out}]$, the fluorescence of safranine T (SAF) increased gradually reaching a level that is stable for at least 60 min (Fig. 6A). The increase of OXO absorbance upon the addition of VAL to vesicles with $[K^+_{in}]<[K^+_{out}]$ was much faster (Fig. 6B). However, the response was less stable than for SAF and about 10–20% of the initial response was lost during the observation time even without the presence of peptide. The observed spectral changes for both potential-sensitive dyes correspond to those described by us previously [28]. The VAL-induced increase of fluorescence (or absorbance) depends linearly on $\Delta\psi$ in the range from +40 to +120 mV (SAF) and from −20 to −120 mV (OXO) as it was reported for small PC vesicles [28].

When TRI or ZER are added to LUVs with a pre-installed $\Delta\psi$, dissipation of the potential is observed and its kinetics appears to be dependent on the initial potential and the peptide concentration (Fig. 6A and B). The depolarisation of a membrane is due to the K^+ efflux and concomitant counterflow of Na^+ leading to equilibration of external and internal concentrations of these ions. The peptide ability to permeate a membrane was quantified by: (1) the initial rate of potential dissipation; (2) the amount of $\Delta\psi$ dissipated during some time period, expressed in percent with respect to the initial $\Delta\psi$ value. For both different peptides, Fig. 7A shows an increase of the initial rate of potential dissipation upon installation of a higher *cis*-positive membrane potential. For example, by an increase of $\Delta\psi$ from +59 to +118 mV, the rate increases by a factor of 5 (for TRI) and 6 (for ZER). This effect cannot be only due to different K^+/Na^+ gradients across a membrane, since the difference $[K^+]_{in}-[K+]_{out}$ (or $[Na^+]_{out}-[Na^+]_{in}$) is only 10% smaller for vesicles with $\Delta\psi=+59$ mV compared to those having $\Delta\psi=+118$ mV. The higher efficiency of TRI (ZER) at elevated *cis*-positive potentials is also demonstrated by the higher levels of vesicle depolarisation that is observed 10 min after peptide addition

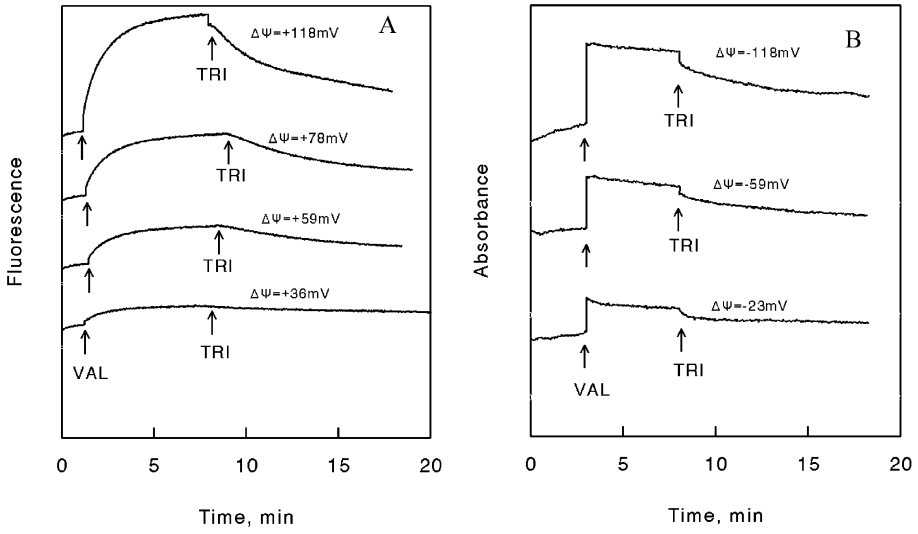

Fig. 6. Dissipation of a transmembrane potential upon addition of TRI to polarised PC vesicles monitored with SAF and OXO as $\Delta\Psi$-sensitive fluorescence absorbance indicators. Panel A (vesicles with *cis*-positive potentials) shows the time dependence of SAF fluorescence in the presence of a K^+-transmembrane gradient with $[K^+]_{in}>[K^+]_{out}$. The PC vesicles contained: inside 200 mM KCl, outside variable KCl and NaCl concentrations (total concentration 200 mM) and at both the in- and outside 10 mM Tris·HCl (pH 7.4). VAL was added to develop a transmembrane potential (indicated near each curve) and subsequently TRI (2.2 μM) was added. $C_{PC}=111$ μM, $C_{VAL}=0.1$ μM, $C_{SAF}=1$ μM; $\lambda_{ex}=520$ nm, $\lambda_{em}=580$ nm. Panel B (vesicles with *cis*-negative potentials) shows the time dependence of the OXO absorbance ($\lambda=617$ nm) in the presence of a K^+-transmembrane gradient with $[K^+]_{in}<[K^+]_{out}$. The PC vesicles contained inside 2 mM KCl, 198 mM NaCl and variable concentrations of KCl and NaCl outside (total concentration 200 mM); both in- and outside concentrations of Tris·HCl are 10 mM (pH 7.4). Subsequently, VAL and TRI were added. $C_{VAL}=0.1$ μM and $C_{TRI}=3.7$ μM. $C_{PC}=172$ μM, $C_{OXO}=1$ μM.

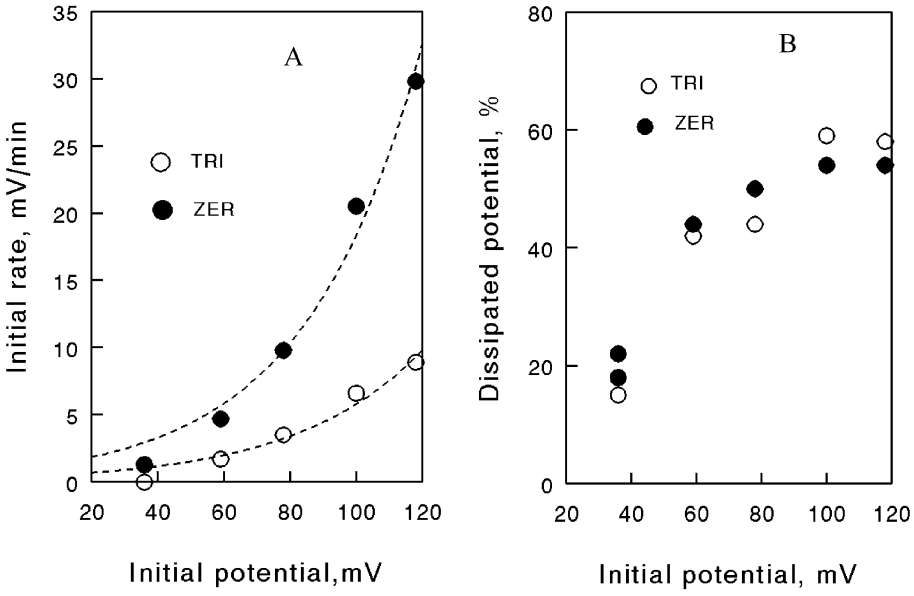

Fig. 7. Effect of the *cis*-positive transmembrane potential $\Delta\psi$ on the peptide-induced depolarisation of vesicles. (A) Dependence of the initial rate of potential dissipation on the magnitude of the initially installed $\Delta\psi$. The initial rate was measured at the linear part of the SAF fluorescence decrease caused by the addition of the same concentration of peptide to vesicles with different magnitudes of initial $\Delta\psi$ (see Fig. 6A for TRI). The fast small initial drop of $\Delta\psi$ was not taken into account and the rate was calculated for the next ~30-s interval. Similar experiments were performed with ZER. The decrease of fluorescence intensity was recalculated into changes of $\Delta\psi$ using the preliminary measured calibration curve (not shown). The dashed lines represent the best exponential fit of the experimental data (see Discussion). (B) The amount of dissipated potential as a function of initially installed potential. The potential dissipated upon peptide addition (10 min after addition) was expressed in percent with respect to the initial value of $\Delta\psi$. For both panels $C_{PC}=111$ μM, $C_{TRI}=2.2$ μM, $C_{ZER}=0.025$ μM.

(Fig. 7B). However, for the negative outside potentials, almost no changes were observed in both TRI- and ZER-activity upon changing the initially installed potential (Fig. 8A and B).

For a given transmembrane potential, independent of its sign, increasing the peptide concentration results in a higher degree of membrane depolarisation (Fig. 9). At all potentials studied, about 100-time lower concentrations of

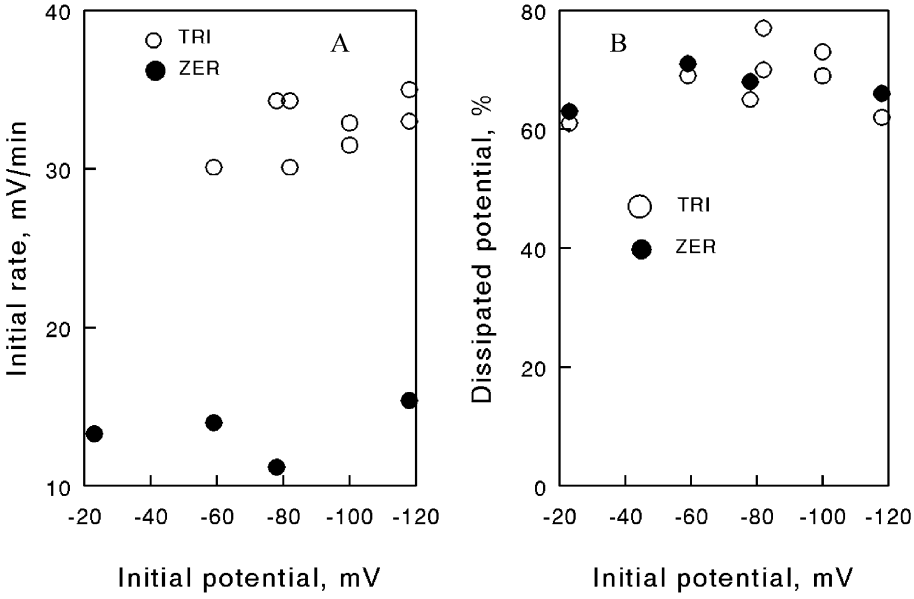

Fig. 8. Effect of the *cis*-negative transmembrane potential $\Delta\psi$ on the peptide-induced depolarisation of vesicles. (A) Dependence of the initial rate of potential dissipation on the magnitude of the previously installed $\Delta\psi$. (B) The amount of dissipated potential as a function of initially installed potential. The rate was monitored as usual (see text under Fig. 7) but using OXO as a $\Delta\psi$-sensitive probe. For both panels $C_{PC}=172$ μM, $C_{TRI}=3.7$ μM, $C_{ZER}=0.033$ μM.

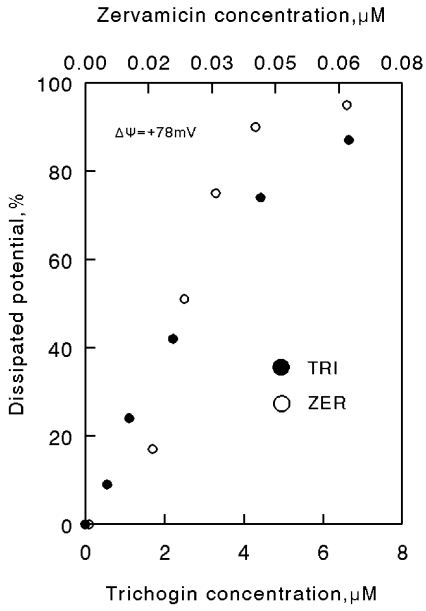

Fig. 9. The amount of dissipated potential as a function of peptide concentration at a constant $\Delta\psi = +78$ mV. The potential dissipated upon addition to polarised PC vesicles (10 min after addition) was expressed in percent with respect to the initial value of $\Delta\psi$. $C_{PC} = 111$ μM.

ZER were required to cause the same effect as that of TRI.

4. Discussion

In the present study the ability of TRI and ZER to cause permeation of monovalent cations (K^+ and Na^+) across the lipid vesicular membrane was shown. The rate constants of the peptaibol-mediated ion transport (Fig. 4) are a few orders of magnitude larger than those for passive ion diffusion through pure membranes. (For a permeability coefficient of monovalent cations in pure membranes being in the range $P = 10^{-14}$–10^{-12} cm/s [31], the calculated rate constant for vesicles with a radius of 450 Å is within the 6.7×10^{-9}–6.7×10^{-7} s^{-1} range).

It was of interest to estimate the number of peptaibol molecules bound per one vesicle capable to cause K^+ leakage. Assuming that the full bilayer thickness (choline-to-choline) for egg PC is ~55 Å and the area occupied by one PC molecule in the bilayer is ~ 70 $Å^2$, for a vesicle with the outer diameter of 900 Å the calculated number of PC molecules per one vesicle is ~ 64,400. Consequently, depending on the peptaibol concentration, one vesicle contains three to nine molecules of ZER. The observed power dependence of the ion diffusion rate on ZER concentrations ($k \sim [\text{Peptide}]^N$), with N in the range 4–7 (Fig. 4), might be an indication of the size of ZER aggregates participating in ion transportation over the examined concentration range. This is in agreement with the molecularity of ZER channels determined from conductivity measurements on planar lipid membranes with 4–16 ZER monomers per channel [9]. Thus, only one or two channels per vesicle are enough to cause complete equilibration of K^+ concentration across a membrane.

A parallel study of both TRI and ZER showed a lower efficiency of the undecapeptide compared to the hexadecapeptide. To get similar effects on the membrane about a 200-fold higher concentrations of TRI were required (Fig. 4). Much larger amounts of TRI (300–2300 TRI molecules per vesicle) necessary for ion transportation make the channel mechanism for this short peptaibol rather unlikely. Though the concentration of membrane-bound TRI is very high, the cooperativity of TRI action is less pronounced ($N = 3$–4), but still showing that some peptide aggregation is involved in ion permeation (see below).

The discrimination in the permeability between K^+ and Na^+ observed in the presence of TRI and ZER is different (Fig. 5, Table 2). Upon addition of TRI a faster permeation was found for K^+ than for Na^+, especially noticeable for low TRI concentrations in the PG membrane. Such behaviour of K^+ and Na^+ corresponds to the relative mobility's of these ions in pure lipid bilayer. The discrimination in K^+/Na^+ permeability by pure lipid membrane is significant for membranes composed of acidic [32] and very unsaturated lipids [33]. The reported ratios of K^+ to Na^+ diffusion rates are 2.4 (PC + 15% phosphatidic acid), 5.4 (PG) and 9.0 (PS) [32].

The preference of K^+ over Na^+ diffusion through a *pure* membrane can be understood, considering the fact that the most likely mechanism for ion transport is permeation through water-filled pores arising from packing defects in the bilayer structure [34]. The probability for an ion to enter such a "statistical pore" is decreased with increasing the size of permeating hydrated ion, thus explaining the observed order: K^+ ($r^+_{K(aq)} = 1.8$ Å)>Na^+ ($r^+_{Na(aq)} = 3.3$ Å). Thus, the preferential permeation of K^+ over Na^+ at low TRI concentrations follows the tendency found for passive diffusion of these ions in pure lipid bilayers. Such finding allows us to suggest that in the presence of a low TRI concentration the principle mechanism of ion permeation is not changed much compared to the pure membrane. However, at higher TRI concentrations, the discrimination between the K^+/Na^+ fluxes becomes smaller (Table 2) and some additional mechanism of ion transport might be operative (see below).

The K^+/Na^+ membrane permeation found in the presence of ZER (Fig. 5B and D, Table 2) is reversed ($Na^+ > K^+$) compared to that mediated by TRI. The observed faster transportation of Na^+ via ZER channels is also different from the permeation sequence found from conductivity measurements for ALA channels ($K^+ > Na^+ > Li^+$) [35,36]. The observed difference in Na^+ and K^+ permeation caused by ZER is weak (rate ratio about 2:1), especially when compared with the permeability ratio P_{Na+}/P_{K+} (~ 14) observed for biological Na^+ channels [37]. The selectivity sequence $Na^+ > K^+$ for ion permeation through a channel is

often the result of a stronger interaction of the ion with the binding sites of the channel compared to ion–water interactions [13,20]. In this respect, it is of interest to compare two characteristic motifs of the respective primary structures of ZER and ALA, i.e. Aib^{7}-X-X-Hyp^{10} and Gly^{11}-X-X-Pro^{14} [38,39]. The molecular structure of ZER shows that, independent of its crystalline [11], solution [12] or micellar bound state [13], the carbonyl of Aib^{7} is at the centre of the concave face of a kinked helix. From the crystal packing [11] and the aggregate structure found in frozen solution [40], it is known that the amphipathic helices are associated to a 'hydrophilic channel like' bundle of antiparallel oriented peptides. In the middle, the channel is closed by two inter-molecular hydrogen bonds between backbone carbonyls (Aib^{7} and Thr^{6} in the respective molecules A and B) and amino acid side chains (the HO-group of Hyp^{10} in molecule B and the amide group of Gln^{11} in A) [11]. After cleavage of the inter-molecular (Aib^{7})C=O. . .HO(Hyp^{10}) hydrogen bond, specific binding of the smaller nonhydrated Na^{+} ion (r^{+}_{Na} = 0.95 Å vs. r^{+}_{K} = 1.33 Å) to the intra-molecular (Aib^{7})C=O. . .N(Hyp^{10}) site can occur which might be a plausible explanation for the observed selectivity of ion conduction. The different ion selectivity observed for ALA might be due to the fact that the Gly^{11}-X-X-Pro^{14} motif of ALA is located just outside the centre of the kinked helical molecule at the wider part of the hydrophilic channel. Thus, for ALA the cation moves through the channel in the hydrated form with the rate proportional to the ion diffusion coefficient in water which depends on its size ($r_{K(aq)}^{+} < r_{Na(aq)}^{+}$).

Since most of the studies on peptaibols membrane activity were performed with planar lipid bilayers, ion conduction was observed under potential-controlled conditions. Contrarily, in vesicular model systems potential-independent ion conduction could be observed for both ZER [28] and ALA [1,6,41,42]. In the present study it was shown that both ZER and TRI could also cause ion permeation through a vesicular membrane in the absence of any transmembrane potential. Thus, the transmembrane voltage is not an obligatory factor for ion transport induced by both studied peptaibols, though installation of a potential (of a proper polarity) indeed increases the peptaibols activity. The potential-independent membrane activity of long-chain peptaibols can be well explained by the existence of an equilibrium between the surface bound and transmembrane orientations of the peptide [43–48]. The amount of the transmembrane state depends on a number of factors including the hydrophobic length of the peptide, the lipid composition, L:P ratio, etc. The 16-residue-long ZER showed a distribution in the orientation when it is bound to DOPC (di-C18:1) or 1,2-dicapryl-*sn*-glycero-3-phosphocholine (di-C10:0) bilayers [47], so that the fraction of transmembrane orientated peptide can participate in channel formation. Contrarily, a transmembrane state for the 11-residue TRI is less likely [45] and even then the helix length (15–16 Å) is not enough to span the bilayer. Recent EPR studies revealed that the TRI helix is bound parallel to the membrane within the lipid head-group region [17]. This mode of binding, together with the insertion of TRI octanoyl tail into the core of the membrane, would perturb the *local* packing of the hydrophobic membrane pocket, thus increasing the amount of "statistical pores" mentioned above. This is similar to the "in-plane diffusion" model suggested in Refs. [46,49] to explain the membrane activity of different peptides. The importance of aliphatic chain insertion for TRI membrane activity was shown by the study of synthetic [Leu^{11}OMe]trichogin GA IV analogues with variable acyl chain lengths (C_2–C_{18}) [16]. The C_{8-10} derivatives were found the most efficient, while C_2 analogue was completely inactive. (However, upon further increasing the chain length of the aliphatic side chain to C_{16-18} atoms, the membrane activity is decreased).

On the other hand, Fig. 4 shows that the ion diffusion rate of TRI is dependent on the on the 3rd–4th power of the TRI concentration, which may indicate that aggregates (trimers and/or tetramers) of TRI are involved in ion permeation. Recently, the aggregation properties of TRI molecules have been studied by means of PELDOR- and CW-EPR spectroscopy as well. In hydrophobic solvents (chloroform and chloroform–toluene mixtures) aggregates containing four peptide molecules are formed, which dissociate upon addition of polar solvents (alcohols) [50,51]. Based on distance measurements between spin labels, incorporated at well-defined positions of the TRI molecules, a 'vesicular' model was proposed for the aggregate composed of four TRI molecules oriented in an antiparallel fashion (the diagonal positioned helices are parallel oriented) [50,51]. The side chains of the apolar amino acid side chains are facing outwards, whereas the polar groups are facing towards a cavity that is closed by both the N-terminal octanoyl groups and the bulky side chains of the C-terminal leucine residues. It might be speculated that at higher concentrations of TRI the solvated ions might be entrapped into this polar pocket of the tetramer formed by association of monomers that are bound at one side of the membrane. After diffusion across the bilayer, the aggregate might dissociate to peptide monomers upon reaching the polar lipid head group region of the other side of the membrane. The length of the octanoyl side chain is supposed to be critical in the formation of opening and closing of the vesicular system, which is in agreement with the observed lack of ion conduction for both short and long aliphatic side chain analogues. It should be noticed that the *microscopic* peptide concentrations used in our experiments, i.e. the concentration of TRI in the membrane phase of the phospholipid vesicles, are in the range of 5–30 mM. This is similar to the concentrations when the equilibrium between monomers and tetramer in hydrophobic solvents was observed [50–52].

The behaviour of TRI and ZER with respect to the transmembrane potential was found to be the same: in LUV both peptides were activated by imposing of *cis*-

positive, but not of *cis*-negative potentials (Figs. 7 and 8). Similar asymmetric current–voltage curves were observed for both Gln^{18} and Glu^{18} analogues of ALA in planar lipid bilayers [2,53,54]. The dissipation of the transmembrane potential, caused by peptide addition (Fig. 6), depends on the peptide-mediated K^+ efflux in exchange for the influx of extravesicular Na^+. Thus, the data presented in Fig. 7A can be interpreted as a voltage dependence of the apparent K^+/Na^+ exchange rate [55]. Similar to the voltage dependence of macroscopic conductance ($G \sim \exp(V/V_e)$, characterised by the V_e—voltage required to produce an e-fold increase in conductance [4,6], the increase of ion transport rate (Fig. 7A) may be approximated with an exponential function. The found values of V_e are practically the same for both peptaibols ($V_e = 34$ mV for ZER and $V_e = 38$ mV for TRI). Compared to the voltage dependence of conductance observed for ZER in planar bilayers with $V_e = 4.5$ mV [9], in vesicular system the voltage activation of ZER is less steep. This resembles the situation with ALA, which is characterised with a V_e value of ~ 20 mV and of 4–9 mV in vesicles and planar bilayers, respectively [2,6,36,53,54].

The observed potential-dependent behaviour of the peptaibols studied can be explained in terms of a voltage-induced insertion/reorientation mechanism (reviewed in Ref. [6]). The peptaibol helix dipole (equivalent with a partial positive and a negative charge at the N- and C-terminus, respectively) causes a reorientation of the peptaibol molecule in the external electric field, so that the fraction of peptaibol oriented perpendicular to the membrane increases. Activation of ZER at *cis*-positive potentials observed in this study as well as before [9,28] shows that insertion of the N-terminus into the bilayer interior is more favourable for channel formation. This binding mode closely resembles that of ALA in which the N-terminus is extended into the central bilayer region even without any transmembrane potential [56–59]. For ZER the higher selectivity for penetration of the N-terminal end into the bilayer is even more likely due to the higher proportion of polar residues at the opposite C-terminal part of the molecule. The deeper insertion of N-terminus compared to the other part of the molecule was also found for ZER bound to a micelle [13]. Thus, the mechanism of voltage activation of both ZER and ALA is better characterised in terms of a pre-orientation/insertion [13] rather than insertion/reorientation model.

In case of TRI, the selective insertion of the N-terminus through the bilayer followed by aggregation and diffusion towards the negatively charged inner surface of the vesicle is initiated by a preferable stabilisation of the octanoyl tail, which is deeply buried into the hydrophobic membrane pocket.

In summary, the present study clearly establishes that the short-chain peptaibol trichogin GA IV can enhance metal ion permeation across phospholipid vesicular membrane. The low membrane activity and the relatively small number of trichogin molecules that are involved in ion translocation seem to exclude the possibility of ion channel formation by this short-chain lipopeptaibol.

Acknowledgements

This investigation project (047.009.018) was financially supported by the Netherlands Organisation for Scientific Research (NWO). We are grateful to Prof. Dr. C. Toniolo and his collaborators for their interest in our investigation.

References

[1] M.K. Mathew, P. Balaram, Mol. Cell. Biochem. 50 (1983) 47–64.
[2] J.E. Hall, I. Vodyanoy, T.M. Balasubramanian, G.R. Marshall, Biophys. J. 45 (1984) 233–247.
[3] G.A. Wooley, B.A. Wallace, J. Membr. Biol. 129 (1992) 109–136.
[4] M.S.P. Sansom, Eur. Biophys. J. 22 (1993) 105–124.
[5] M.S.P. Sansom, Q. Rev. Biophys. 26 (1993) 365–421.
[6] D.S. Cafiso, Annu. Rev. Biophys. Biomol. Struct. 23 (1994) 141–265.
[7] A.D. Argoudelis, A. Dietz, L.E. Johnson, J. Antibiot. 27 (1974) 321–328.
[8] S. Agarwalla, I.R. Mellor, M.S.P. Sansom, I.L. Karle, J.L. Flippen-Anderson, K. Uma, K. Krishna, M. Sukumar, P. Balaram, Biochem. Biophys. Res. Commun. 186 (1992) 8–15.
[9] P. Balaram, K. Krishna, M. Sukumar, I.R. Mellor, M.S.P. Sansom, Eur. Biophys. J. 21 (1992) 117–128.
[10] M.S.P. Sansom, P. Balaram, I.L. Karle, Eur. Biophys. J. 21 (1993) 369–383.
[11] I.L. Karle, J.L. Flippen-Anderson, S. Agarwalla, P. Balaram, Proc. Natl. Acad. Sci. U. S. A. 88 (1991) 5307–5311.
[12] T.A. Balashova, Z.O. Shenkarev, A.A. Tagaev, T.V. Ovchinnikova, J. Raap, A.S. Arseniev, FEBS Lett. 466 (2000) 333–336.
[13] Z.O. Shenkarev, T.A. Balashova, R.G. Efremov, Z.A. Yakimenko, T.V. Ovchinnikova, J. Raap, A.S. Arseniev, Biophys. J. 82 (2002) 762–771.
[14] C. Auvin-Guette, S. Rebuffat, Y. Prigent, B. Bodo, J. Am. Chem. Soc. 114 (1992) 2170–2174.
[15] C. Toniolo, M. Crisma, F. Formaggio, C. Peggion, R.F. Epand, R.M. Epand, Cell. Mol. Life Sci. 68 (2001) 1179–1188.
[16] C. Toniolo, M. Crisma, F. Formaggio, C. Peggion, V. Monaco, C. Goulard, S. Rebuffat, B. Bodo, J. Am. Chem. Soc. 118 (1996) 4952–4958.
[17] V. Monaco, F. Formaggio, M. Crisma, C. Toniolo, P. Hanson, G.L. Millhauser, Biopolymers 50 (1999) 239–253.
[18] R.M. Epand, Y. Shai, J.P. Segrest, G.M. Anantharamaiah, Biopolymers 37 (1995) 319–338.
[19] Z. Orenm, Y. Shai, Biopolymers 47 (1998) 451–463.
[20] G. Eisenman, R. Horn, J. Membr. Biol. 76 (1983) 197–225.
[21] M.J. Hope, M.B. Bally, G. Webb, P.R. Cullis, Biochim. Biophys. Acta 812 (1985) 55–65.
[22] P.S. Chen, T.Y. Toribara, H. Warner, Anal. Chem. 28 (1956) 1756–1758.
[23] T.A. Egorova-Zachernuk, V.I. Shvets, K. Versluis, W. Heerma, A.F.L. Creemers, S.A.M. Nieuwenhuis, J. Lugtenburg, J. Raap, J. Pept. Sci. 2 (1996) 341–350.
[24] P. Jezek, F. Mahdi, K.D. Garlid, J. Biol. Chem. 265 (1990) 10522–10526.
[25] A. Minta, R.Y. Tsien, J. Biol. Chem. 264 (1989) 19449–19457.
[26] A.D. Bangham, M.M. Standish, J.C. Watkins, J. Mol. Biol. 13 (1965) 238–252.
[27] G.A. Woolley, M.K. Kapral, C.M. Deber, FEBS Lett. 224 (1987) 337–342.

[28] T.N. Kropacheva, J. Raap, FEBS Lett. 460 (1999) 500–504.
[29] J.J. Schuurmans, R.P. Casey, R. Kraayenhof, FEBS Lett. 94 (1978) 405–409.
[30] H.S. van Walraven, K. Krab, M.J.M. Hagendoorn, R. Kraayenhof, FEBS Lett. 184 (1985) 96–99.
[31] R.B. Gennis, Biomembranes, Molecular Structure and Function, Springer-Verlag, New York, 1989.
[32] D. Papahadjopoulos, Biochim. Biophys. Acta 241 (1971) 254–259.
[33] A. Scarpa, J. de Gier, Biochim. Biophys. Acta 241 (1971) 789–797.
[34] D.W. Deamer, J. Bramhall, Chem. Phys. Lipids 40 (1986) 167–188.
[35] W. Hanke, G. Boheim, Biochim. Biophys. Acta 596 (1980) 456–462.
[36] M. Eisenberg, J.E. Hall, C.A. Mead, J. Membr. Biol. 14 (1973) 143–176.
[37] B. Hille, Ion Channels of Excitable Membranes, Sinauer Associates, Inc., Massachussets, 1992, p. 351.
[38] M.S. Sansom, Prog. Biophys. Mol. Biol. 55 (1991) 139–235.
[39] J. Jacob, H. Duclohier, D.S. Cafiso, Biophys. J. 67 (1994) 1861–1866.
[40] A.D. Milov, Yu.D. Tsvetkov, E.Yu. Gorbunova, L.G. Mustaeva, T.V. Ovchinnikova, J. Raap, Biopolymers 64 (2002) 328–336.
[41] G.A. Woolley, C.M. Deber, Biopolymers 28 (1989) 267–272.
[42] M. Dathe, C. Kaduk, E. Tachikawa, M. Melzig, H. Wenschuh, M. Bienert, Biochim. Biophys. Acta 1370 (1998) 175–183.
[43] H.W. Huang, Y. Wu, Biophys. J. 60 (1991) 1079–1087.
[44] H.W. Huang, Biochemistry 39 (2000) 8347–8352.
[45] W.T. Heller, K. He, S.J. Ludtke, T.A. Harroun, H.W. Huang, Biophys. J. 73 (1979) 239–244.
[46] B. Bechinger, J. Membr. Biol. 156 (1997) 197–211.
[47] B. Bechinger, D.A. Skladnev, A. Ogrel, X. Li, E.V. Rogozhkina, T.V. Ovchinnikova, J.D.J. O'Neil, J. Raap, Biochemistry 30 (2001) 9428–9437.
[48] U. Harzer, B. Bechinger, Biochemistry 39 (2000) 13106–13114.
[49] B. Bechinger, Biochem. Biophys. Acta 1462 (1999) 157–183.
[50] A.D. Milov, Yu.D. Tsvetkov, F. Formaggio, M. Crisma, C. Toniolo, J. Raap, J. Am. Chem. Soc. 122 (2000) 3843–3848.
[51] A.D. Milov, Yu.D. Tsvetkov, F. Formaggio, M. Crisma, C. Toniolo, J. Raap, J. Am. Chem. Soc. 123 (2001) 3784–3789.
[52] A.D. Milov, Yu.D. Tsvetkov, F. Formaggio, M. Crisma, C. Toniolo, G.L. Millhauser, J. Raap, J. Phys. Chem., B 105 (2001) 11206–11213.
[53] I. Vodyanoy, J.E. Hall, T.M. Balasubramanian, Biophys. J. 42 (1983) 71–82.
[54] S.J. Archer, D.S. Cafiso, Biophys. J. 60 (1991) 380–388.
[55] X. Chen, R.V. Gross, Biochemistry 33 (1994) 13769–13774.
[56] R.O. Fox, F.M. Richards, Nature (Lond.) 300 (1982) 325–330.
[57] M. Barranger-Mathys, D.S. Cafiso, Biochemistry 35 (1996) 498–505.
[58] C.L. North, M. Barranger-Mathys, D.S. Cafiso, Biophys. J. 69 (1995) 2392–2397.
[59] D.P. Tieleman, M.S.P. Sansom, H.J.C. Berendsen, Biophys. J. 76 (1999) 40–49.